CrossMark

Patch-based fuzzy clustering for image segmentation

Xiaofeng Zhang[1,2] · **Qiang Guo[2]** · **Yujuan Sun[1]** · **Hui Liu[2]** · **Gang Wang[1]** · **Qingtang Su[1]** · **Caiming Zhang[1,2]**

Abstract
Fuzzy C-means has been adopted for image segmentation, but it is sensitive to noise and other image artifacts due to not considering neighbor information. In order to solve this problem, many improved algorithms have been proposed, such as fuzzy local information C-means clustering algorithm (FLICM). However, the segmentation results of FLICM are unsatisfactory when performed on complex images. To overcome this, a novel fuzzy clustering algorithm is proposed in this paper, and more information is utilized to guide the procedure of image segmentation. In the proposed algorithm, pixel relevance based on patch similarity will be investigated firstly, by which all information over the whole image can be considered, not limited to local context. Compared with Zhang et al. (Multimed Tools Appl 76(6):7869–7895, 2017a. https://doi.org/10.1007/s11042-016-3399-x) pixel relevance is unnecessary to be normalized, and much more information can play positive role in image segmentation. Experimental results show that the proposed algorithm outperforms current fuzzy algorithms, especially in enhancing the robustness of corresponding fuzzy clustering algorithms.

Keywords Image segmentation · Fuzzy clustering · FLICM · Pixel relevance · Patch similarity

1 Introduction

Image segmentation is the core technology of image processing, analysis, recognition and understanding (Sun et al. 2016a, b; Zhu et al. 2016a, b). With the development of Inter-net, information processing and related areas, many topics are relevant to image processing (Li et al. 2014a, b, 2017b, d). The success of many topics, such as object recognition, video surveillance, depends on accurate segmentation (Huang et al. 2017; Li et al. 2017c). Also, image segmentation emerges in new areas such as copy–move forgery detection (Li et al. 2017a), in which the test image is segmented into semantically independent patches prior to keypoint extraction, and the copy–move regions can be detected by matching between these patches. In essence, image segmentation is to group the pixels in the given image into different clusters according to their features. In many cases, the given image is complex, and many kinds of artifacts exist. When the pixels are contaminated by noise, the feature values of the pixels will be affected greatly, and conventional segmentation algorithms perform poor. To the best of our knowledge, there are no segmentation algorithms that can be performed on images of any kind. Also, in other complex images such as medical images, the feature values of pixels are not the true values due to the imaging principle. In medical images, the intensity of pixels is the average value of the pixels locating in the same slice, which may belong to different organs or tissues (Ji et al. 2010, 2011). Therefore, conventional "hard" methods that assign the pixel to one organ or tissue are not suitable to segment complex images due to the relevance between

✉ Xiaofeng Zhang
  iamzxf@126.com

  Qiang Guo
  qguo@sdu.edu.cn

  Yujuan Sun
  syj_anne@163.com

  Hui Liu
  liuh_lh@126.com

  Gang Wang
  happy_wg@163.com

  Qingtang Su
  sdytsqt@163.com

  Caiming Zhang
  czhang@sdu.edu.cn

[1] School of Information and Electrical Engineering, Ludong University, Yantai 254025, China

[2] School of Computer Science and Technology, Shandong University of Finance and Economics, Jinan 250014, China

neighbor pixels. In this paper, fuzzy clustering approaches will be investigated, because they can admit one pixel to several classes concurrently and can retain information as much as possible.

Fuzzy C-means, abbreviated as FCM, is a typical fuzzy clustering algorithm which is simple and efficient. It was proposed by Dunn (1974) and later extended by Bezdek (1981). In FCM, only pixel intensity is considered, and as a result, FCM is sensitive to noise and other image artifacts (Pham and Prince 1999; Pham 2001). Aiming at this problem, many improved versions were proposed. In these improved algorithms, neighbor information is introduced into the objective function, and the segmentation results are improved greatly. However, when used in complex images with high-level noise, these improved algorithms still perform poor, and the reason is that only information in the neighbor window is utilized. In our opinion, all information in the given image should be utilized, not limited to local ones (Zhao et al. 2011a, b; Zhao 2013). For example, there are many pixels with similar neighborhood configuration to one given pixel and can be utilized to enhance the robustness of the algorithm. These pixels may exist far from the given pixel and cannot be considered in the improved algorithms mentioned above (Liu et al. 2015; Gong et al. 2013). In this paper, the information provided by the neighbor pixels is called local information, while that provided by the pixels far from the given pixel is called non-local information. In this paper, one improved fuzzy algorithm is proposed, which can be divided into two phases. In the first phase, the model of pixel relevance between different pixels is investigated. Based on pixel relevance, non-local information is incorporated into fuzzy clustering algorithm in the second phase, which can enhance the robustness to noise and image artifacts.

The rest of the paper is organized as follows. Section 2 introduces the related algorithms, including conventional fuzzy C-means algorithm and typical improved ones. The model of pixel relevance is proposed in Sect. 3, and then one improved algorithm based on non-local information and fuzzy clustering algorithm is proposed. Section 4 presents the corresponding experiments of the proposed algorithm on different images, and one short but important conclusion is drawn in the last section.

2 Related works

2.1 Conventional fuzzy C-means algorithm

Fuzzy C-means is a typical clustering algorithm in pattern recognition and machine learning, the target of which is to minimize the weighted distance between pixels and cluster centers. In FCM, the objective function is defined as

$$F = \sum_{i=1}^{C} \sum_{j=1}^{n} u_{ij}^m d_{ij}^2, \tag{1}$$

where n is the number of pixels in the given image, C is the predefined number of clusters, and $u_{ij} \in [0, 1]$ is the membership of the jth pixel belonging to the ith cluster, satisfying $\sum_{i=1}^{C} u_{ij} = 1$. $m > 1$ is a parameter to control the fuzziness of the clustering results. $d_{ij} = \|x_j - v_i\|$, where x_j is the intensity value of the jth pixel and v_i is the value of the ith cluster center. To minimize the objective function with the constraints, Lagrange multiplier method is adopted, and the following function will be created.

$$J = \sum_{i=1}^{C} \sum_{j=1}^{n} u_{ij}^m d_{ij}^2 + \sum_{j=1}^{n} \lambda_j \left(\sum_{i=1}^{C} u_{ij} - 1 \right). \tag{2}$$

Based on $\frac{\partial J}{\partial u_{ij}} = 0$ and $\frac{\partial J}{\partial v_i} = 0$, the update equations of the cluster centers and the memberships will be deduced as follows.

$$u_{ij} = \frac{\|x_j - v_i\|^{-2/(m-1)}}{\sum_{k=1}^{C} \|x_j - v_k\|^{-2/(m-1)}}, \tag{3}$$

$$v_i = \frac{\sum_{j=1}^{n} u_{ij}^m x_j}{\sum_{j=1}^{n} u_{ij}^m}. \tag{4}$$

If $\max\{|u_{ij}^{p+1} - u_{ij}^p|\} < \varepsilon$ holds or the predefined number of iterations is satisfied, the procedure will be terminated, in which ε is the predefined threshold. Then the maximum membership procedure method will be adopted to retrieve the segmentation results, which will assign the jth pixel to the kth class with the highest membership.

As shown in Eq. (1), only intensity information is utilized in FCM. As a result, FCM is sensitive to noise and cannot retrieve good results in complex images. To solve this problem, many improved algorithms were proposed in relevant literature, and several typical ones are illustrated as follows.

2.2 FCM-related algorithms

To make fuzzy clustering algorithms more robust, many improved algorithms were proposed, such as bias-corrected version of FCM (denoted as BCFCM) (Ahmed et al. 2002), BCFCMS1 and BCFCMS2 (Chen and Zhang 2004), enhanced FCM (denoted as EnFCM) (Szilágyi et al. 2003), fast generalized fuzzy C-means clustering (denoted as FGFCM) (Cai et al. 2007) and fuzzy local information C-means algorithm (denoted as FLICM) (Krinidis and Chatzis 2010). In these improved algorithms, various spatial information is added to the objective function of FCM. For example, in FLICM, a fuzzy factor has been added to reflect the impact of neighbor information, which is defined as follows.
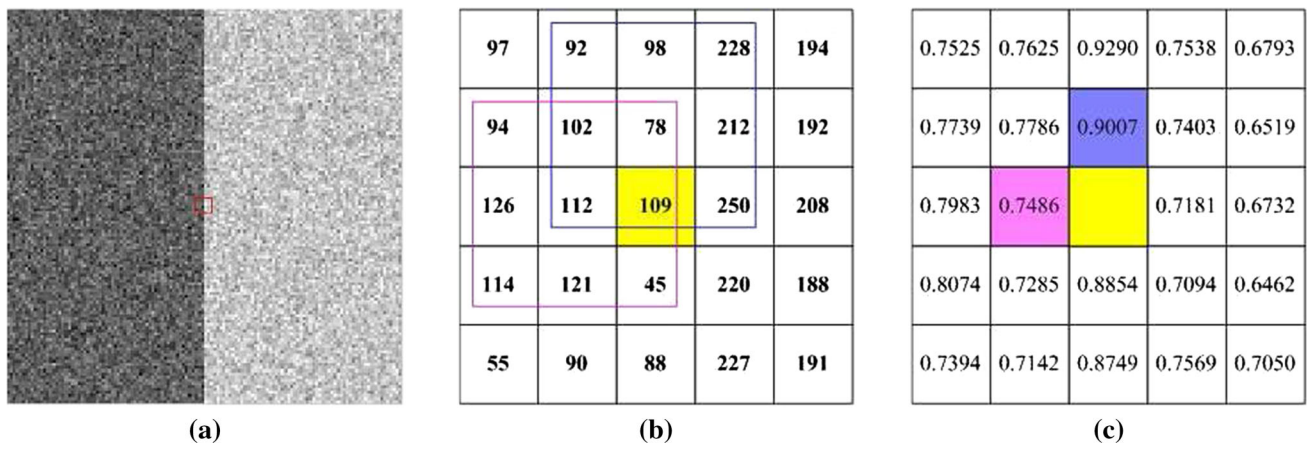
Fig. 1 Pixel relevance between neighbor pixels and the central one. **a** Image with noise; **b** intensities of pixels in the red box; **c** pixel relevance between the central pixel and the neighbor pixels (color figure online)
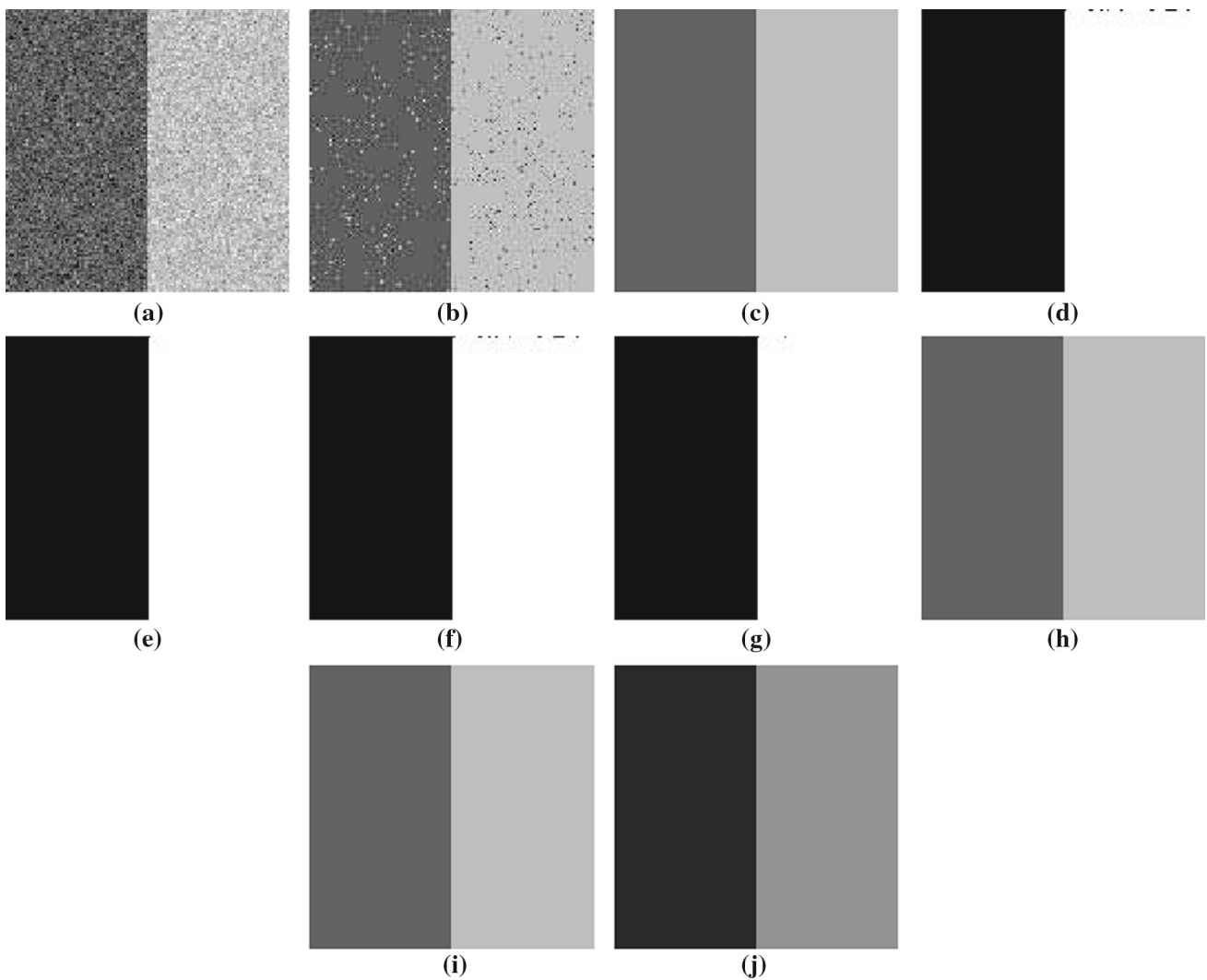

Fig. 2 Segmentation results of the first synthetic image. **a** Noisy image corrupted by Gaussian noise of level 20%. **b** FCM result. **c** BCFCM result. **d** BCFCMS1 result. **e** BCFCMS2 result. **f** EnFCM result. **g** FGFCM result. **h** FLICM result. **i** KWFLICM result. **j** PRFLICM result
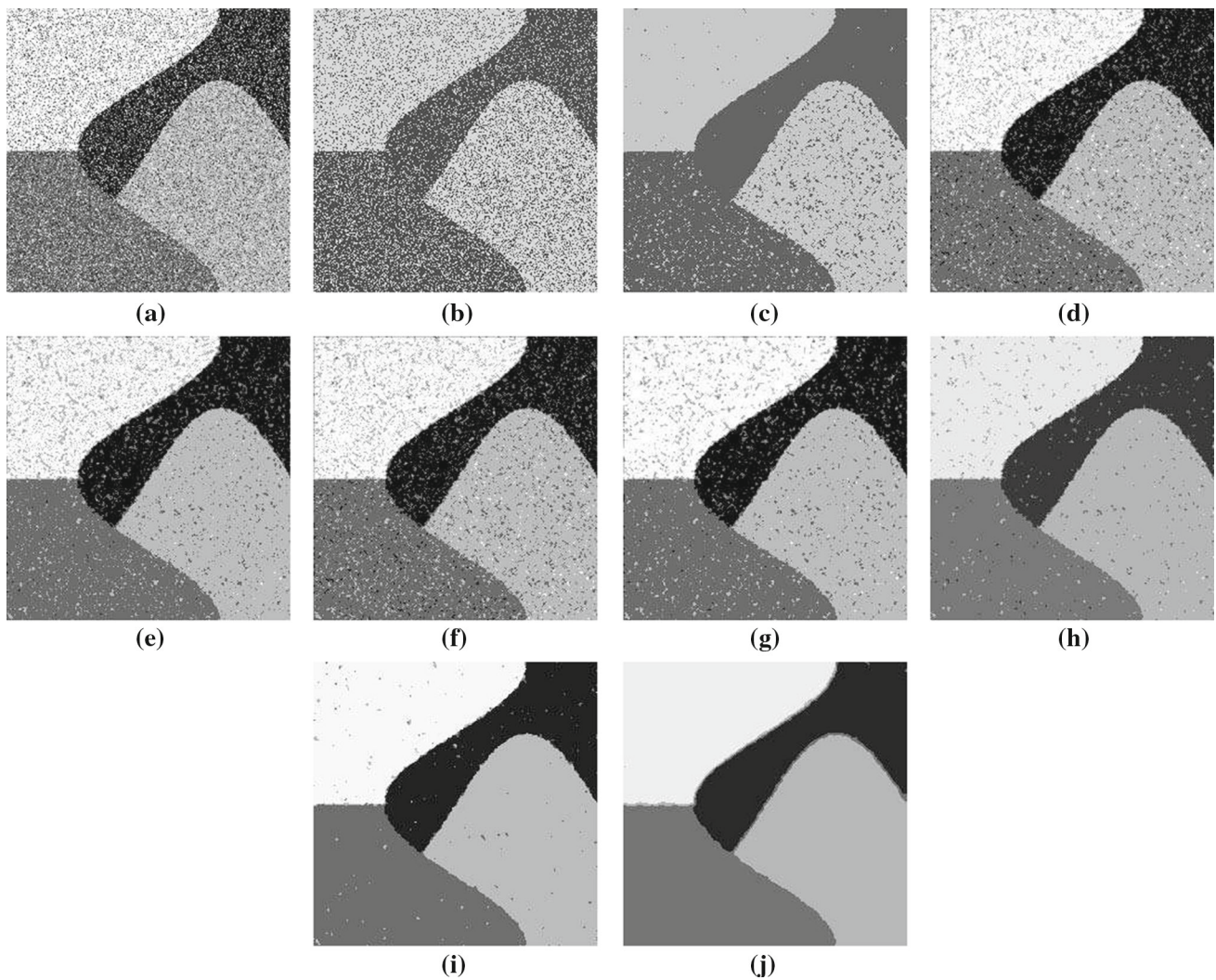
Fig. 3 Segmentation results of the second synthetic image. **a** Noisy image corrupted by Salt&Pepper noise of level 30%. **b** FCM result. **c** BCFCM result. **d** BCFCMS1 result. **e** BCFCMS2 result. **f** EnFCM result. **g** FGFCM result. **h** FLICM result. **i** KWFLICM result. **j** PRFLICM result

$$G_{ij} = \sum_{r \in N_j} \frac{1}{d_{jr} + 1} (1 - u_{ir})^m \|x_r - v_i\|^2. \tag{5}$$

With the help of G_{ij}, the corresponding membership values of the all pixels that falling into the local window will converge to a similar value, including noisy pixels and non-noisy ones (Gong et al. 2013). By adding the fuzzy factor, the objective function of FLICM can be defined as

$$F = \sum_{i=1}^{C} \sum_{j=1}^{n} \left[u_{ij}^m (x_j - v_i)^2 + G_{ij} \right]. \tag{6}$$

Also, the objective function is minimized with the constraints $\sum_{i=1}^{C} u_{ij} = 1 (j = 1, 2, \ldots, n)$. Using Lagrange multiplier method, the memberships and cluster centers can be updated as follows.

$$u_{ij} = \frac{1}{\sum_{k=1}^{C} \left(\frac{\|x_j - v_i\|^2 + G_{ij}}{\|x_j - v_k\|^2 + G_{kj}} \right)^{1/(m-1)}}, \tag{7}$$

$$v_i = \frac{\sum_{j=1}^{n} u_{ij}^m x_j}{\sum_{j=1}^{n} u_{ij}^m}. \tag{8}$$

Though the robustness of FCM can be improved with the help of the spatial information, these improved algorithms perform poor when the image is complex or the noise level is high. This paper holds the idea that the reason for such poor performance is that only the spatial information of local window is utilized. However, there is much information that can be utilized in the procedure of image segmentation. For example, there are many pixels with similar configurations to the given pixel, not limited to local context. However,

Table 1 SA (%) on the first synthetic image with different noises

Noise	FCM	BCFCM	BCFCMS1	BCFCMS2	EnFCM	FGFCM	FLICM	KWFLICM	PRFCM
Gaussian 15%	97.854	99.986	99.975	99.981	99.975	99.994	99.969	99.988	99.996
Gaussian 20%	97.571	99.986	99.913	99.986	99.913	99.988	99.945	99.982	99.988
Gaussian 30%	97.351	99.988	99.851	99.988	99.857	99.986	99.786	99.878	99.988
Salt&Pepper 15%	92.572	94.214	94.259	95.914	94.184	99.070	99.652	99.951	99.954
Salt&Pepper 20%	89.777	91.681	92.107	94.519	91.754	98.345	99.206	99.902	99.945
Salt&Pepper 30%	84.570	85.822	85.790	90.508	85.783	94.265	99.231	99.780	99.801

Table 2 Comparison of partition coefficient V_{pc} on the synthetic images with different noise

Image	Noise	FCM	BCFCM	BCFCMS1	BCFCMS2	EnFCM	FGFCM	FLICM	KWFLICM	PRFLICM
Fig. 2	Gaussian 15%	0.8993	0.8902	0.9430	0.9468	0.9707	0.9770	0.9114	0.9490	0.9850
	Gaussian 20%	0.8970	0.8884	0.9413	0.9449	0.9692	0.9750	0.9102	0.9484	0.9849
	Gaussian 30%	0.8957	0.8855	0.9389	0.9434	0.9672	0.9737	0.9091	0.9475	0.9844
	Salt&Pepper 15%	0.9556	0.7572	0.8864	0.9463	0.9287	0.9782	0.9037	0.9615	0.9622
	Salt&Pepper 20%	0.9381	0.6934	0.8543	0.9260	0.9112	0.9658	0.8748	0.9486	0.9478
	Salt&Pepper 30%	0.8747	0.5835	0.7887	0.8827	0.8779	0.9365	0.8040	0.9213	0.9622
Fig. 3	Gaussian 15%	0.8833	0.8777	0.8090	0.8112	0.9584	0.8658	0.8493	0.9455	0.9512
	Gaussian 20%	0.8864	0.8792	0.9090	0.8029	0.9497	0.8585	0.7200	0.9410	0.9514
	Gaussian 30%	0.8872	0.8723	0.8720	0.8813	0.9256	0.9024	0.7599	0.9061	0.9111
	Salt&Pepper 15%	0.8658	0.7874	0.8122	0.8802	0.8875	0.9464	0.7261	0.8445	0.9206
	Salt&Pepper 20%	0.8645	0.7600	0.7594	0.8378	0.8591	0.9183	0.6478	0.7927	0.9186
	Salt&Pepper 30%	0.8628	0.6999	0.6551	0.7385	0.8104	0.8569	0.4863	0.6745	0.8712

Table 3 Comparison of partition entropy V_{pe} on the synthetic images with different noise

Image	Noise	FCM	BCFCM	BCFCMS1	BCFCMS2	EnFCM	FGFCM	FLICM	KWFLICM	PRFLICM
Fig. 2	Gaussian 15%	0.2594	0.3110	0.1700	0.1652	0.0919	0.0778	0.2564	0.1558	0.0457
	Gaussian 20%	0.2641	0.3152	0.1742	0.1700	0.0956	0.0833	0.2591	0.1573	0.0460
	Gaussian 30%	0.2667	0.3215	0.1797	0.1731	0.1003	0.0859	0.2617	0.1594	0.0449
	Salt&Pepper 15%	0.1264	0.5390	0.2802	0.1155	0.1906	0.0569	0.2585	0.1022	0.1020
	Salt&Pepper 20%	0.1731	0.6677	0.3490	0.1589	0.2292	0.0876	0.3232	0.1352	0.0704
	Salt&Pepper 30%	0.3099	0.8684	0.4868	0.2545	0.3042	0.1621	0.4757	0.2035	0.1043
Fig. 3	Gaussian 15%	0.3023	0.3301	0.5563	0.5474	0.1597	0.4120	0.4833	0.1877	0.1517
	Gaussian 20%	0.2885	0.3181	0.2812	0.5633	0.1601	0.4253	0.8026	0.1997	0.1482
	Gaussian 30%	0.2697	0.3083	0.3621	0.3363	0.2357	0.2441	0.6836	0.2810	0.2279
	Salt&Pepper 15%	0.3566	0.5178	0.5482	0.3375	0.3377	0.2690	0.8157	0.4864	0.2567
	Salt&Pepper 20%	0.3557	0.5683	0.6873	0.4569	0.4132	0.3502	1.01638	0.6326	0.3323
	Salt&Pepper 30%	0.5537	0.6768	0.9521	0.7278	0.5375	0.5281	1.4081	0.9482	0.5233

these pixels are located far away from the given pixel and cannot be considered in the improved algorithms mentioned above. To overcome this, one improved clustering algorithm is presented in this paper, the starting point of which is to replace the local information with non-local information.

3 Pixel relevance

In the algorithms mentioned in Sect. 2, the impact of spatial information on the central pixel is weighted by one parameter, such as α in BCFCM and EnFCM, S_{ij} in FGFCM and
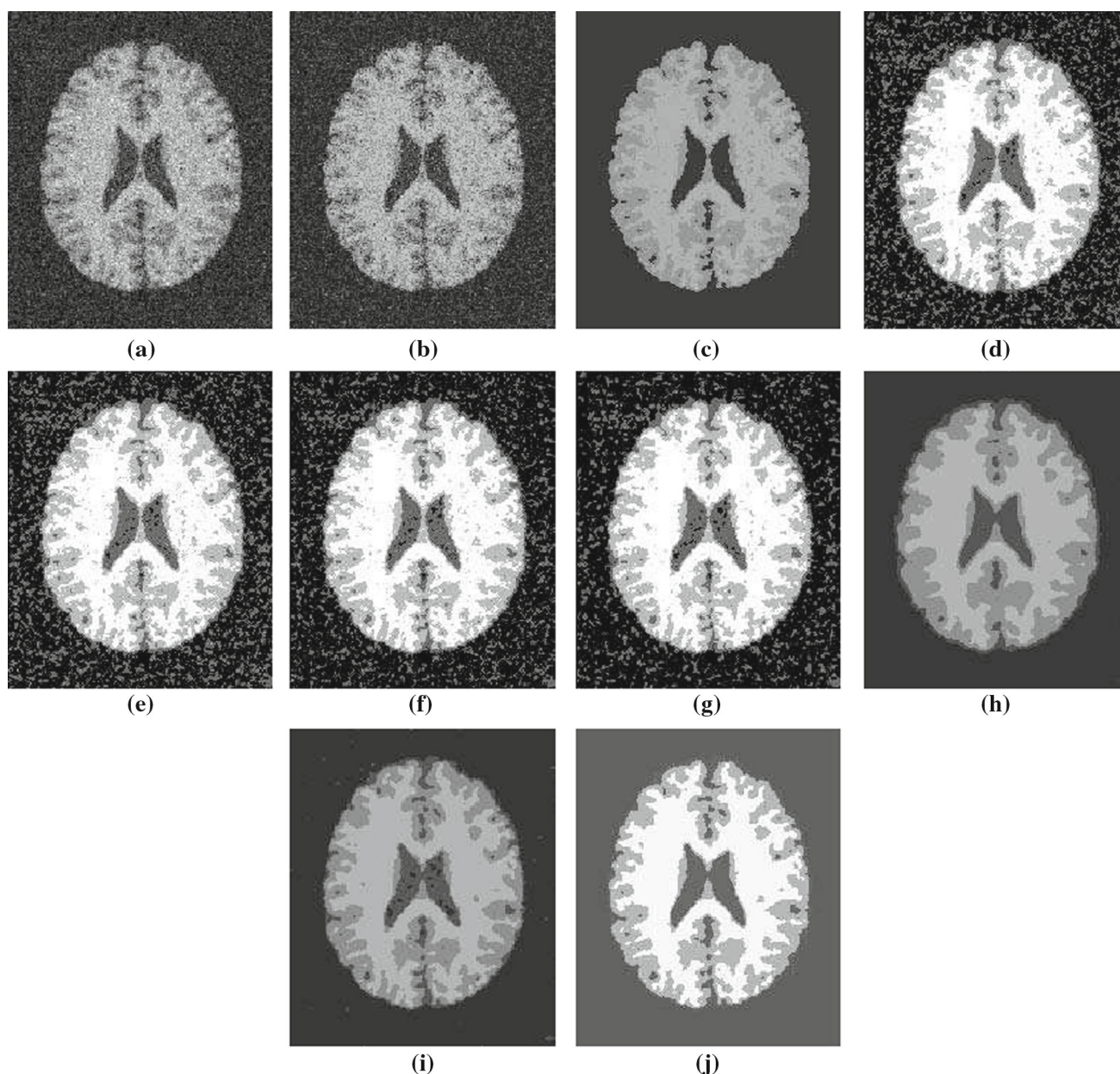
Fig. 4 Segmentation results of one medical image corrupted by 30% Rician noise. **a** Noisy image corrupted by Rician noise of level 30%. **b** FCM result. **c** BCFCM result. **d** BCFCMS1 result. **e** BCFCMS2 result. **f** EnFCM result. **g** FGFCM result. **h** FLICM result. **i** KWFLICM result. **j** PRFLICM result

the fuzzy factor G_{ij} in FLICM. As analyzed in Buades et al. (2008) and Zhang et al. (2012), this impact can be seen as pixel relevance between neighbor pixel and the central one. If pixel relevance between neighbor pixels is more accurate, much better results can be retrieved. However, pixel relevance in these improved algorithms cannot reflect the true relation between pixels. For example, pixel relevance in BCFCM is assigned as a constant, and this setting leads to a blurring effect near the edges. When the noise level is high, current improved algorithms cannot perform well. In Zhang et al. (2017a, b), we found that the statistical information is

insensitive to image artifacts. Therefore, we will construct an image patch centering the given pixel, and pixel relevance will be measured by using the similarity of corresponding image patches.

Given two pixels i and j, two image patches N_i and N_j centering around the two pixels are constructed, and the pixel relevance between the two pixels is defined as

$$S(i, j) = 1 - \frac{\sum_{p=1}^{|N_i|} \left| N_i^p - N_j^p \right|}{|N_i| * 255}, \tag{9}$$
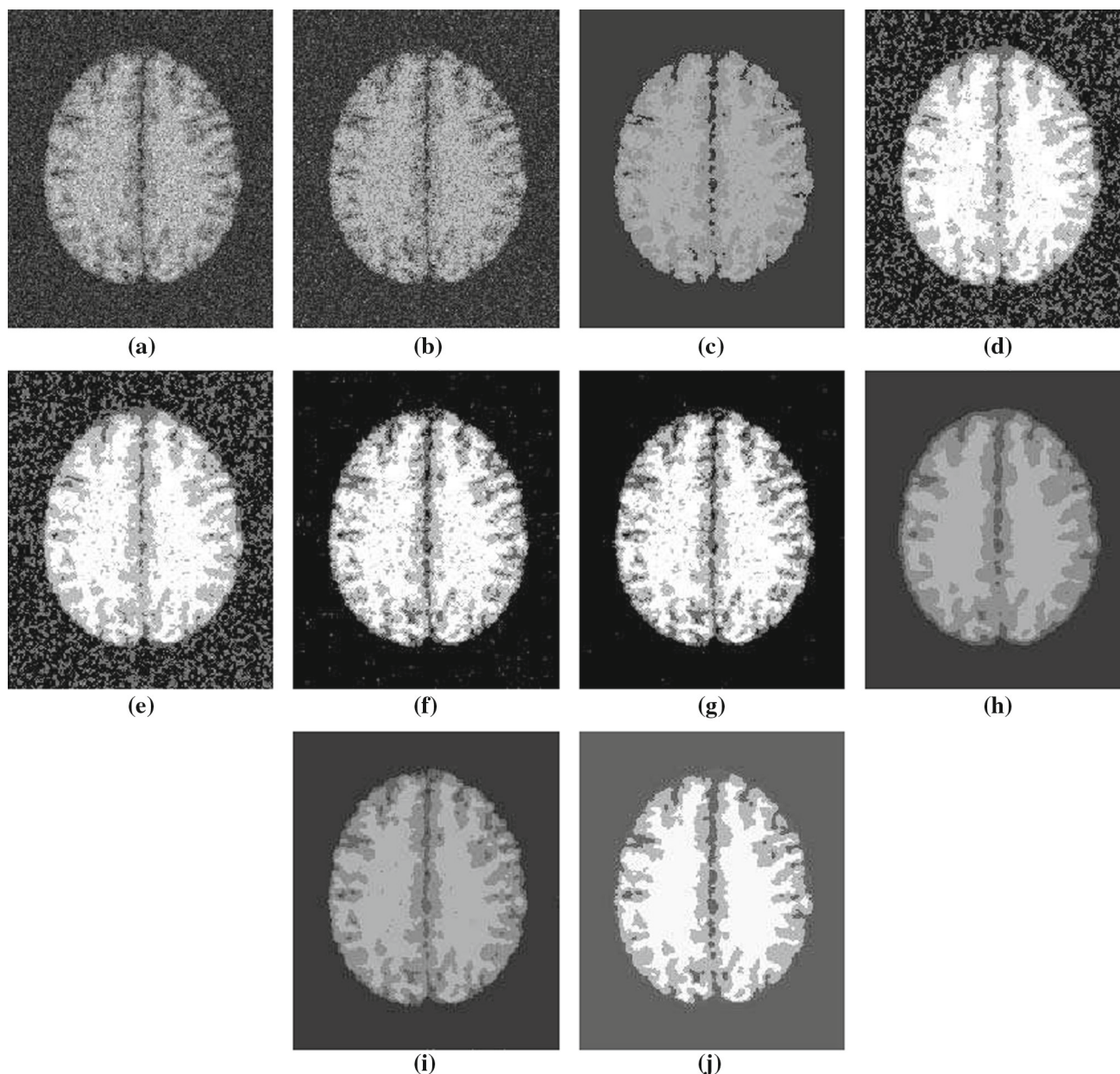
Fig. 5 Segmentation results of another medical image corrupted by 30% Rician noise. **a** Noisy image corrupted by Rician noise of level 30%. **b** FCM result. **c** BCFCM result. **d** BCFCMS1 result. **e** BCFCMS2 result. **f** EnFCM result. **g** FGFCM result. **h** FLICM result. **i** KWFLICM result. **j** PRFLICM result

where $|N_i|$ is the cardinality of N_i and N_i^p is the pth value of image patch N_i. The constructed image patches are often with different geometrical structures due to the positions of pixels. In order to compute pixel relevance accurately, the geometrical structures of N_i and N_j are desired to be the same, which can make our algorithm more robust to image artifacts. As shown in Eq. (9), if the two image patches are the same, $S(i, j)$ is equal to 1. The more similar the two patches are, the closer $S(i, j)$ is to 1, and vice versa.

We take one example shown in Fig. 1a to illustrate the computation of pixel relevance. The intensities of pixels in the red box are tabulated in Fig. 1b, and corresponding pixel relevances between the central pixel (in yellow) and the considered pixels are presented in Fig. 1c. According to Eq. (9), the value of pixel relevance between the central pixel and the neighbor pixels depends on the similarity between corresponding image patches. As is shown in Fig. 1c, pixel relevance between the pixel with intensity value 78 and the central pixel is larger than that between the pixel with intensity value 112 and the central pixel, even though the intensity value of the central pixel is closer to the pixel with intensity value 112, larger than the pixel with intensity value 78.
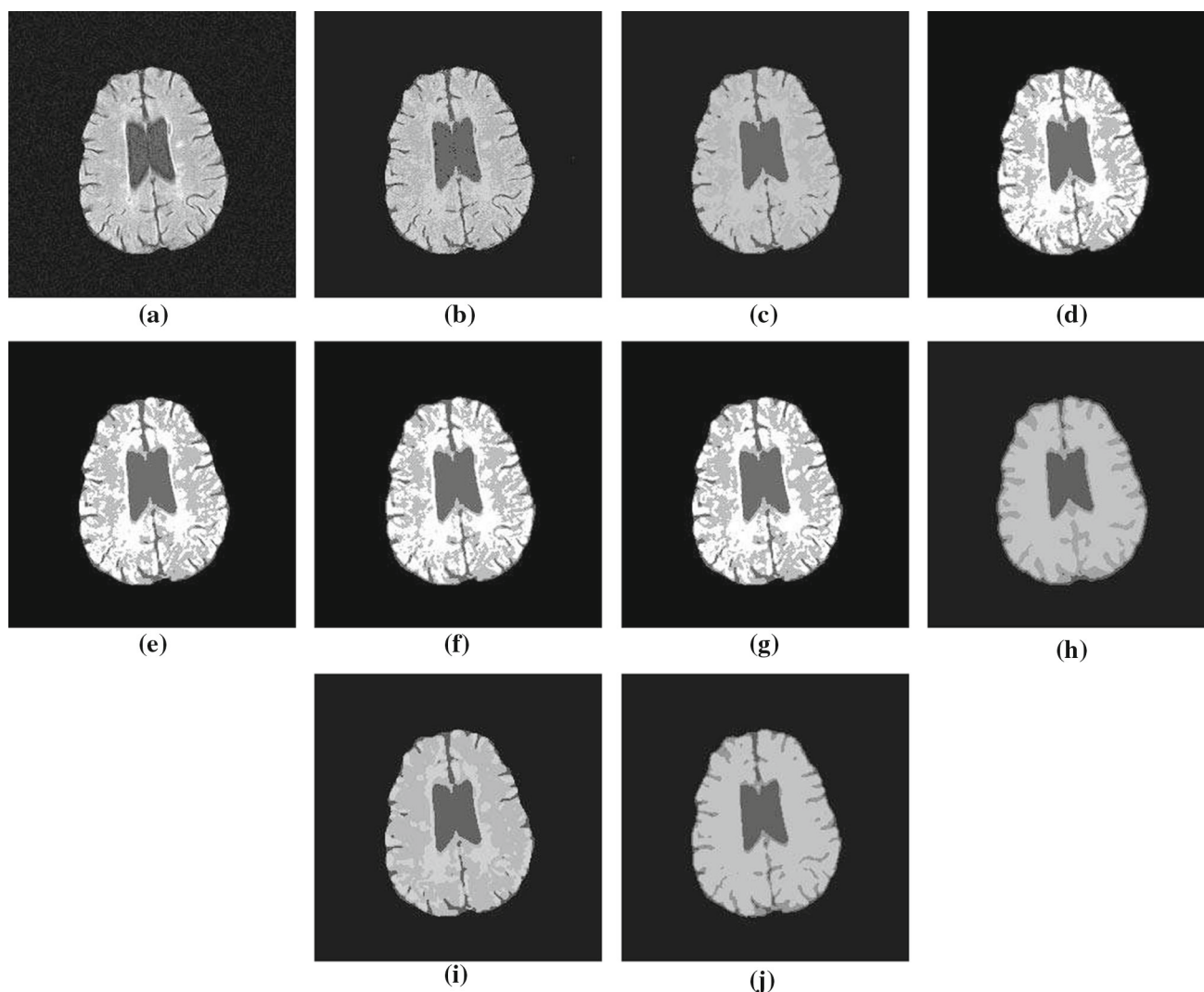
Fig. 6 Segmentation results of another medical image corrupted by 30% Rician noise. **a** Noisy image corrupted by Rician noise of level 10%. **b** FCM result. **c** BCFCM result. **d** BCFCMS1 result. **e** BCFCMS2 result. **f** EnFCM result. **g** FGFCM result. **h** FLICM result. **i** KWFLICM result. **j** PRFLICM result

Compared with previous work (Zhang et al. 2017a), pixel relevance is unnecessary to be normalized in this paper. The reason is that when non-local information is considered, all information in the search window will be utilized. When the pixel relevance is normalized, many pixel relevance values will be close to 0, which makes the non-local information play low role in the procedure of image segmentation.

With the help of pixel relevance, more information can be utilized in the procedure of image segmentation, not limited to local window. However, considering more information means low efficiency. To balance the segmentation results and efficiency, one search window will be defined, and only the pixels in the search window with similar configurations will play positive role in guiding image segmentation. In this paper, the search window centering around the ith pixel will be denoted as W_i^r, where r is the radius. In the following

experiments, r is assigned as 3, meaning that the size of W_i is 7×7.

4 Proposed algorithm

Based on the analysis mentioned above, this section will introduce pixel relevance into the objective function of the proposed algorithm. For a pixel, the pixels with higher relevance will have similar membership, playing positive role in the procedure of image segmentation. That is to say, if $S(i, j)$ is big, the damping extent of the jth pixel on the ith pixel should be big, and vice versa. Then the membership of the pixels with higher relevance will converge to similar values and in turn enhance the robustness of the proposed algorithm. Therefore, the fuzzy factor in the proposed algorithm can be defined as follows.

Table 4 Comparison of V_{pc} and V_{pe} on medical images with Rician noise (30%)

Parameter	Image	FCM	BCFCM	BCFCMS1	BCFCMS2	EnFCM	FGFCM	FLICM	KWFLICM	PRFLICM
V_{pc}	Fig. 4	0.7775	0.4538	0.6606	0.6600	0.8054	0.8054	0.7698	0.7143	0.8183
	Fig. 5	0.7741	0.4513	0.6450	0.6481	0.8469	0.8558	0.6263	0.7301	0.8621
	Fig. 6	0.9195	0.8581	0.9105	0.9142	0.9344	0.9366	0.9271	0.9170	0.9483
V_{pe}	Fig. 4	0.6050	1.3171	0.8673	0.8697	0.5190	0.5171	0.6468	0.8208	0.5002
	Fig. 5	0.6138	1.3246	0.8952	0.8916	0.4391	0.4174	0.9193	0.7819	0.3955
	Fig. 6	0.2363	0.3848	0.2466	0.2382	0.1789	0.1723	0.2036	0.2366	0.1523

Table 5 Comparison of SAs for brain images with Rician noise (30%)

Image	Region	FCM	BCFCM	BCFCMS1	BCFCMS2	EnFCM	FGFCM	FLICM	KWFLICM	PRFLICM
Fig. 4	CSF	0.7533	0.7810	0.8139	0.8057	0.8451	0.8562	0.9430	0.9452	0.9459
	GRY	0.8167	0.5685	0.9137	0.9114	0.9113	0.9153	0.9286	0.9234	0.9288
	WHT	0.8620	0.9368	0.9470	0.9419	0.9486	0.9501	0.9462	0.9557	0.9588
Fig. 5	CSF	0.7248	0.7471	0.7552	0.7516	0.9422	0.9402	0.9490	0.9495	0.9497
	GRY	0.8213	0.9205	0.9172	0.9144	0.8836	0.8768	0.9230	0.9123	0.9238
	WHT	0.8682	0.9413	0.9483	0.9461	0.9351	0.9376	0.9498	0.9540	0.9597

$$G_{ij} = \sum_{k \in W_j^r} S(j,k)(1 - u_{ik})^m \|x_k - v_i\|^2. \tag{10}$$

Considering pixel relevance is utilized in the improved algorithm, the proposed algorithm is denoted as PRFLICM, and the framework is illustrated in Algorithm 1.

Algorithm 1 The framework of PRFLICM.

Step 1. Compute pixel relevance between pixel i and $j \in W_i^r$ by Eq.(9);
Step 2. Initialize the fuzzy partition matrix u^0 at random;
Step 3. Set the iterator counter $it = 1$;
Step 4. Compute cluster centers by Eq.(8);
Step 5. Compute the fuzzy factor by Eq.(10);
Step 6. Update the fuzzy partition matrix u^{it} by Eq.(7);
Step 7. If $max\{|u^{it} - u^{it-1}|\} < \varepsilon$ or $it = maxIter$ holds, go to Step 8, else $it = it + 1$, go to Step 4;
Step 8. Assign the jth pixel to the kth cluster, where $k = \arg\{\max u_{kj}\}$.

---

5 Experiments and analysis

In order to verify the effectiveness of our algorithm, the comparison of the segmentation results will be performed between the proposed algorithm and the competing algorithms, including FCM, FCMS, FCMS1, FCMS2, FGFCM, EnFCM, FLICM and KWFLICM. Corresponding parameters in the related algorithms are assigned as follows: $m = 2$, $\varepsilon = 1e-5$ and 3×3 neighborhood is adopted for local search. α is assigned to 2 in BCFCM, FCMS1, FCMS2 and EnFCM. λ_G and λ_S are assigned to 2 and 3 in FGFCM, respectively.

Also, three evaluation criteria have been adopted to compare the algorithms.

(1) Segmentation accuracy (SA) is defined as the sum of the correctly classified pixels divided by the number of all pixels. Formally,

$$\text{SA} = \sum_{i=1}^{C} \frac{A_i \cap C_i}{\sum_{j=1}^{C} C_j}, \tag{11}$$

where A_i is the set of pixels belonging to the ith class; C_i is the set of pixels belonging to the ith class in the reference image.

(2) Partition coefficient V_{pc} (Bezdek 1975a) is one validity function to evaluate the algorithms, defined as

$$V_{\text{pc}} = \sum_{i=1}^{C} \sum_{j=1}^{n} u_{ij}^2 / n. \tag{12}$$

(3) Partition entropy V_{pe} (Bezdek 1975b) is another validity function to evaluate the clustering algorithms, defined as

$$V_{\text{pe}} = -\sum_{i=1}^{C} \sum_{j=1}^{n} \left(u_{ij} \log u_{ij}\right) / n, \tag{13}$$

where n is the number of pixels in the given image.

Obviously, one good algorithm should have higher SAs and less fuzziness, and the latter means bigger V_{pc} and smaller V_{pe}.
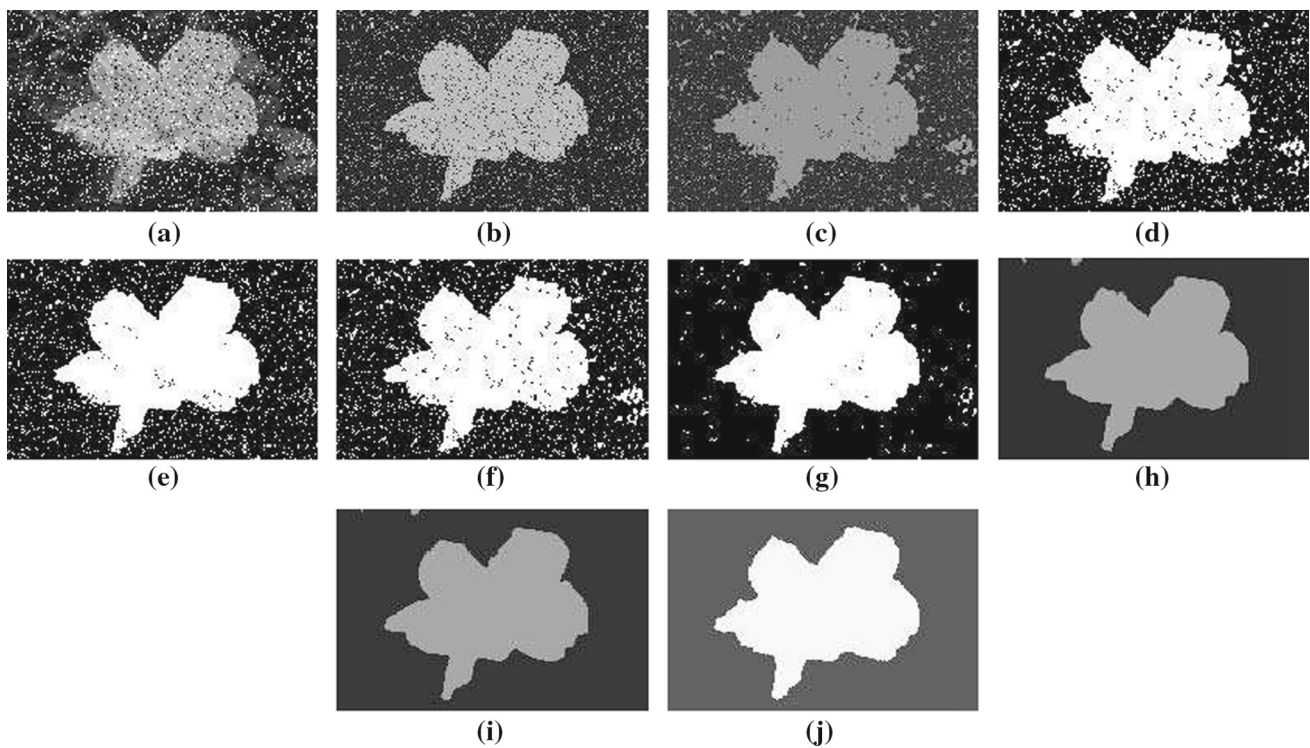
Fig. 7 Segmentation results of the first natural image. **a** Noisy image corrupted by Salt&Pepper noise of level 15%. **b** FCM result. **c** BCFCM result. **d** BCFCMS1 result. **e** BCFCMS2 result. **f** EnFCM result. **g** FGFCM result. **h** FLICM result. **i** KWFLICM result. **j** PRFLICM result
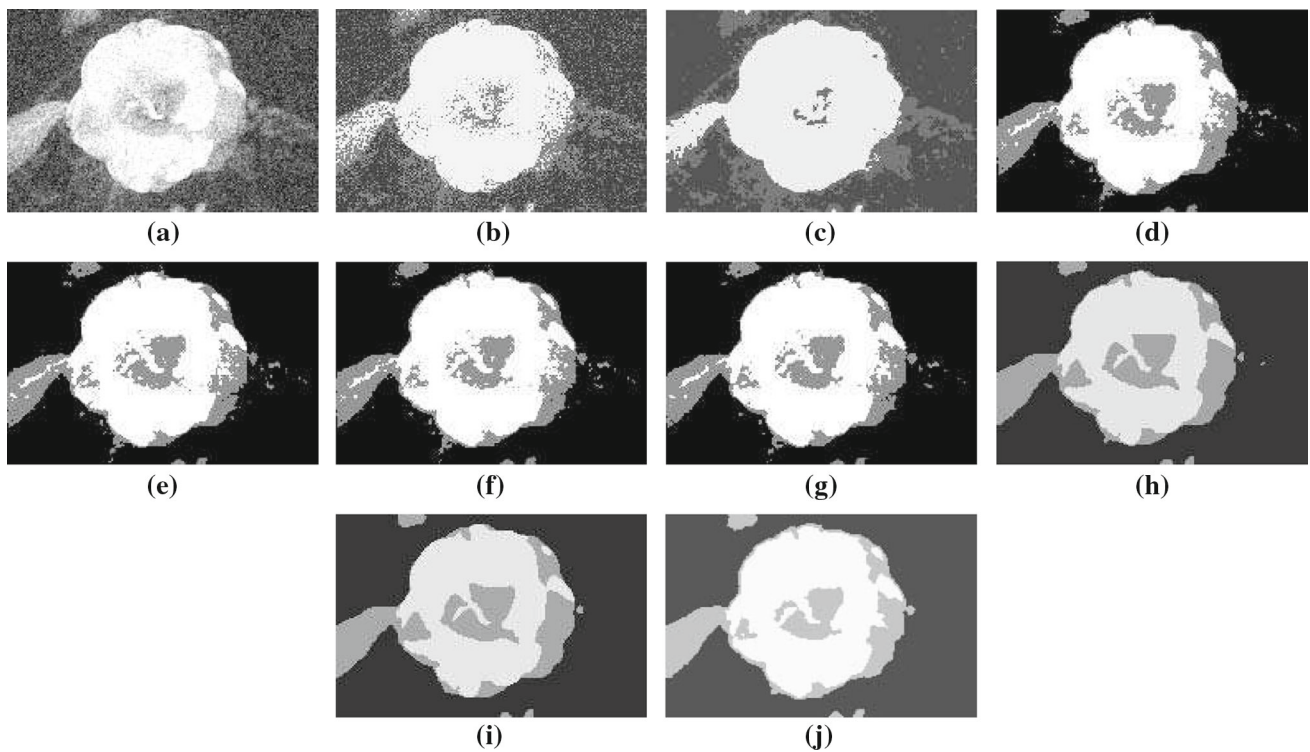

Fig. 8 Segmentation results of the second natural image. **a** Noisy image corrupted by Gaussian noise of level 15%. **b** FCM result. **c** BCFCM result. **d** BCFCMS1 result. **e** BCFCMS2 result. **f** EnFCM result. **g** FGFCM result. **h** FLICM result. **i** KWFLICM result. **j** PRFLICM result
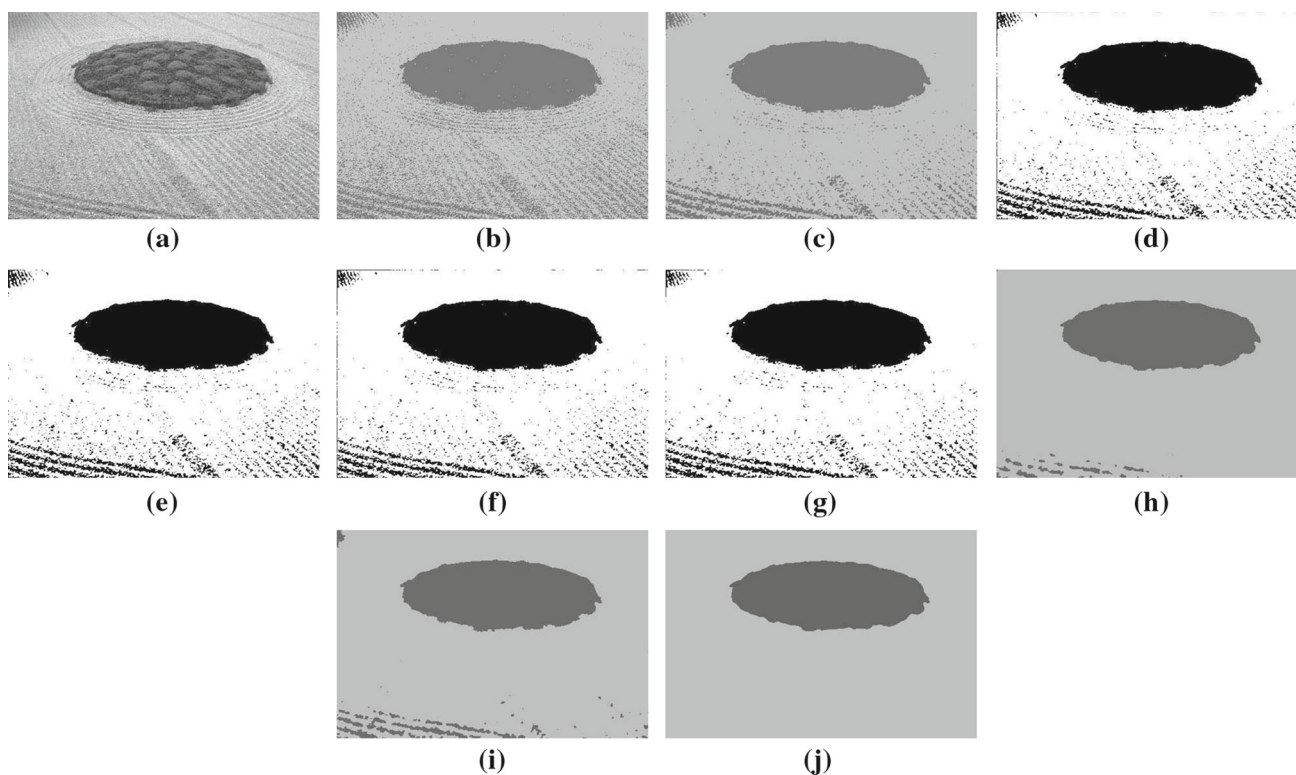
Fig. 9 Segmentation results of the third natural image. **a** Original image. **b** FCM result. **c** BCFCM result. **d** BCFCMS1 result. **e** BCFCMS2 result. **f** EnFCM result. **g** FGFCM result. **h** FLICM result. **i** KWFLICM result. **j** PRFLICM result

Table 6 Comparison of V_{pc} and V_{pe} on natural images

Parameter	Image	FCM	BCFCM	BCFCMS1	BCFCMS2	EnFCM	FGFCM	FLICM	KWFLICM	PRFLICM
V_{pc}	Fig. 7	0.9244	0.7444	0.8675	0.9089	0.9050	0.9395	0.9023	0.9473	0.9668
	Fig. 8	0.8201	0.6810	0.8582	0.8617	0.8905	0.8955	0.9123	0.8845	0.9262
	Fig. 9	0.8513	0.7942	0.8607	0.8590	0.8867	0.8883	0.9596	0.9189	0.9626
V_{pe}	Fig. 7	0.2026	0.5737	0.3262	0.2250	0.2426	0.1623	0.2495	0.1438	0.0978
	Fig. 8	0.4678	0.7773	0.3965	0.3879	0.3046	0.2917	0.2422	0.3364	0.2103
	Fig. 9	0.3596	0.4950	0.3490	0.3531	0.2855	0.2826	0.1175	0.2236	0.1139

5.1 Experiments on synthetic images

The first experiment is performed on two synthetic images. To illustrate the advantage of the proposed algorithm, various noise is added to the image: the first image is with Gaussian noise of 20% level, and the second image is with Salt&Pepper noise of 30% level. The segmentation results of corresponding algorithms are illustrated in Figs. 2 and 3.

As shown in Figs. 2 and 3, image artifacts still exist in the results of FCM, BCFCMS1, BCFCMS2, EnFCM and FGFCM, and all noise is removed by BCFCM, FLICM, KWFLICM and PRFLICM. Also, we compare the SAs of these algorithms on the first synthetic image with different noise, tabulated in Table 1.

As listed in Table 1, the SAs of the proposed algorithm are higher than those of the other improved algorithms. Also, the values of V_{pc} and V_{pe} are compared, shown in Tables 2 and 3. It is to be noted that the V_{pc} and V_{pe} values are the average values of 10 runs.

As tabulated in Tables 2 and 3, the partition coefficients and the partition entropies of the proposed algorithm are better than those of the other algorithms, meaning that considering pixel relevance to guide the procedure of image segmentation is reasonable. Moreover, the two parameters of PRFLICM are more stable, comparable to those of KWFLICM and better than the other algorithms.

5.2 Experiments on medical images

PRFLICM is performed further on three medical images, including 2 magnetic resonance (MR) images from Brain-Web images (Buades et al. 2008) and one computed tomography (CT) image from Krinidis and Chatzis (2010). As introduced in Gong et al. (2013), medical images are often contaminated with Rician noise. In our experiments, the first two images are corrupted by 30% Rician noise ($s = 30$) MathWorks, and the third image is corrupted by 10%. The number of clusters is predefined as 4, and the segmentation results of the nine algorithms are presented in Figs. 4b–j, 5b–j and 6b–j.

As shown in Figs. 4, 5 and 6, noise still exists in the results of FCM, BCFCM, FCMS1, FCMS2, FGFCM, EnFCM, a small portion of noise exists in the results of KWFLICM, and almost all noise is removed by FLICM and PRFLICM.

To compare these algorithms quantitatively, V_{pc} and V_{pe} are adopted, and corresponding values on these three images are tabulated in Table 4. As shown, PRFLICM has the best V_{pc} and V_{pe}, meaning that the membership values in the proposed algorithm are more crisp.

Moreover, the task of image segmentation for brain images is to partition the image into four parts: background, cerebral spinal fluid (CSF), gray matter (GRY) and white matter (WHT). Compared with the referenced images of BrainWeb (Buades et al. 2008), the SAs on CSF, GRY and WHT of the nine algorithms are presented in Table 5. As shown from Table 5, the segmentation accuracy of PRFLICM is higher than that of the other algorithms, meaning that our algorithm can segment different tissues accurately.

5.3 Experiments on natural images

In this subsection, the proposed algorithm is performed on three natural images, two from Besser (1990), and the other is from Krinidis and Chatzis (2010). The number of clusters of the three images is predefined as 2, 3 and 2. To compare the results with other algorithms, the first two figures are contaminated with Salt&Pepper noise (15%) and Gaussian noise (15%), and the third figure is to retrieve the saliency region. The segmentation results of the nine algorithms on the three natural images are presented in Figs. 7b–j, 8b–j and 9b–j.

V_{pc} and V_{pe} are compared in our experiments, and the results are presented in Table 6. As shown from Table 6, more crisp membership values are obtained by PRFLICM, resulting in higher V_{pc} and smaller V_{pe}.

6 Conclusions and future work

In this paper, an improved clustering algorithm is proposed for image segmentation. In our algorithm, based on the fact that statistical information is insensitive to image artifacts, image patches are constructed centering corresponding pixels, and pixel relevance is measured based on the similarity of corresponding image patches. With the help of pixel relevance, non-local information is added into the procedure of image segmentation. Then, more information can be utilized to guide the procedure of image segmentation, which can improve the robustness of the proposed algorithm. Experiments on synthetic, medical and natural images show that our algorithm outperforms other FCM-related algorithms. However, the selection of the radius of search window is a key issue for the proposed algorithm. The large radius will be adopted to resist the effect of high-level noise, while a small one will be done to resist the effect of low-level noise. In addition, the boundaries of the segmentation results may be blurred, shown in Figs. 3 and 8. Hence how to select the radius of the search window to balance the segmentation effect and efficiency should be investigated in the future work, which will also deblur the boundaries of the segmentation results.

Compliance with ethical standards

Conflict of interest All of the authors declare that they have no conflict of interest.

References

Ahmed MN, Yamany SM, Mohamed N, Farag AA (2002) A modified fuzzy C-mean algorithm for bias field estimation and segmentation of MRI data. IEEE Trans Med Imaging 21(3):193–199

Besser H (1990) Visual access to visual images: the UC Berkeley image database project. Libr Trends 38(4):787–798

Bezdek JC (1975a) Cluster validity with fuzzy sets. J Cybern 3(3):58–73

Bezdek JC (1975b) Mathematical models for systematics and taxonomy. In: Proceedings of eighth international conference on numerical taxonomy, vol 3, pp 143–166

Bezdek J (1981) Pattern recognition with fuzzy objective function algorithms. Plenum, New York

Buades A, Coll B, Morel JM (2008) Nonlocal image and movie denoising. Int J Comput Vis 76(2):123–139

Cai W, Chen S, Zhang D (2007) Fast and robust fuzzy C-means clustering algorithms incorporating local information for image segmentation. Pattern Recognit 40:825–838

Chen S, Zhang D (2004) Robust image segmentation using FCM with spatial constraints based on new kernel-induced distance measure. IEEE Trans Syst Man Cybern B Cybern 34:1907–1916

Cocosco CA, Kollokian V, Kwan RKS et al Brainweb: online interface to a 3D MRI simulated brain database. http://www.bic.mni.mcgill.ca/brainweb/

Dunn J (1974) A fuzzy relative of the isodata process and its use in detecting compact well separated clusters. J Cybern 3:3257

Gong M, Liang Y, Shi J, Ma W, Ma J (2013) Fuzzy C-means clustering with local information and kernel metric for image segmentation. IEEE Trans Image Process 22(2):573–584

Huang Z, Liu S, Mao X, Chen K, Li J (2017) Insight of the protection for data security under selective opening attacks. Inf Sci. https://doi.org/10.1016/j.ins.2017.05.031

Ji Z, Sun Q, Xia D (2010) A modified possibilistic fuzzy C-means clustering algorithm for bias field estimation and segmentation of brain MR image. Comput Med Imaging Gr 35:383–397

Ji X, Sun Q, Xia D (2011) A framework with modified fast FCM for brain MR images segmentation. Pattern Recognit 44:999–1013

Krinidis S, Chatzis V (2010) A robust fuzzy local information C-means clustering algorithm. IEEE Trans Image Process 19(5):1328–1337

Li J, Chen X, Li M, Li J, Lee PPC, Lou W (2014a) Secure deduplication with efficient and reliable convergent key management. IEEE Trans Parallel Distrib Syst 25(6):1615–1625

Li J, Huang X, Li J, Chen X, Xiang Y (2014b) Securely outsourcing attribute-based encryption with checkability. IEEE Trans Parallel Distrib Syst 25(8):2201–2210

Li J, Li X, Yang B, Sun X (2017a) Segmentation-based image copy–move forgery detection scheme. IEEE Trans Inf Forensics Secur 10(3):507–518

Li J, Yan H, Liu Z, Chen X, Huang X, Wong DS (2017b) Location-sharing systems with enhanced privacy in mobile online social networks. IEEE Syst J. https://doi.org/10.1109/JSYST.2015.2415835

Li P, Li J, Huang Z, Li T, Gao C, Yiu S-M, Chen K (2017c) Multi-key privacy-preserving deep learning in cloud computing. Future Gener Comput Syst. https://doi.org/10.1016/j.future.2017.02.006

Li P, Li J, Huang Z, Gao C-Z, Chen W, Chen K (2017d) Privacy-preserving outsourced classification in cloud computing. Clust Comput. https://doi.org/10.1007/s10586-017-0849-9

Liu H, Zhang C, Su ZY, Wang K, Deng K (2015) Research on a pulmonary nodule segmentation method combining fast self-adaptive FCM and classification. Comput Math Methods Med. https://doi.org/10.1155/2015/185726

MathWorks. Image processing toolbox, natick,ma. http://www.mathworks.com/matlabcentral/fileexchange/14237

Pham DL (2001) Spatial models for fuzzy clustering. Comput Vis Image Underst 84(2):285–297

Pham DL, Prince JL (1999) An adaptive fuzzy C-means algorithm for image segmentation in the presence of intensity inhomogeneities. Pattern Recognit Lett 20(1):57–68

Sun Y, Jian M, Zhang X, Dong J, Shen L, Chen B (2016a) Reconstruction of normal and albedo of convex Lambertian objects by solving ambiguity matrices using SVD and optimization method. Neurocomputing 207:95–104

Sun Z, Zhang Q, Li Y, Tan Y-A (2016b) Dppdl: a dynamic partial-parallel data layout for green video surveillance storage. IEEE Trans Circuits Syst Video Technol. https://doi.org/10.1109/TCSVT.2016.2605045

Szilágyi L, Benyó Z, Szilágyii SM, Adam HS (2003) MR brain image segmentation using an enhanced fuzzy C-means algorithm. In: Proceeding of 25th annual international conference of IEEE EMBS, vol 34, pp 17–21

Zhang X, Zhang C, Tang W, Wei Z (2012) Medical image segmentation using improved FCM. Sci China Inf Sci 55(4):1052–1061

Zhang X, Sun Y, Wang G, Guo Q, Zhang C, Chen B (2017a) Improved fuzzy clustering algorithm with non-local information for image segmentation. Multimed Tools Appl 76(6):7869–7895. https://doi.org/10.1007/s11042-016-3399-x

Zhang X, Wang G, Qingtang S, Guo Q, Zhang C, Chen B (2017b) An improved fuzzy algorithm for image segmentation using peak detection, spatial information and reallocation. Soft Comput 21(8):2165–2173. https://doi.org/10.1007/s00500-015-1920-1

Zhao F (2013) Fuzzy clustering algorithms with self-tuning non-local spatial information for image segmentation. Neurocomputing 106:115–125

Zhao F, Jiao L, Liu H (2011a) Fuzzy C-means clustering with non local spatial information for noisy image segmentation. Front Comput Sci China 5(1):45–56

Zhao F, Jiao L, Liu H, Gao X (2011b) A novel fuzzy clustering algorithm with non local adaptive spatial constraint for image segmentation. Signal Process 91:988–999

Zhu R, Tan Y-A, Zhang Q, Li Y, Zheng J (2016a) Determining image base of firmware for ARM devices by matching literal pools. Dig Investig 16:19–28

Zhu R, Tan Y-A, Zhang Q, Wu F, Zheng J, Xue Y (2016b) Determining image base of firmware files for ARM devices. IEICE Trans Inf Syst E99D(2):351–359